Chapter

Polycrystalline Diamond Characterisations for High End Technologies

Awadesh Kumar Mallik

Abstract

Characterisations of polycrystalline diamond (PCD) coatings have routinely been done over the past three decades of diamond research, but there is less number of reports on some of its very unique properties. For example, diamond is the hardest known material and, in probing such hard surfaces with any indenter tip, it may lead to damage of the instrument. Due to such chances of experimental accidents, researchers have performed very few attempts in evaluating the mechanical properties of PCDs. In the present work, some of these very special properties of diamond that are less reported in the literature are being re-investigated. PCDs were characterised by photoluminescence (PL), Fourier transform infrared (FTIR) spectroscopy, transmission electron microscope (TEM), and X-ray diffraction (XRD) techniques. The diamond surface was also polished to bring the as-grown micron level of surface roughness (detrimental for wear application) down to few hundreds of nanometer. The tribological properties of such polished and smooth surfaces were found to be appropriate for wear protective coating application. This chapter revisits some of the unreported issues in the synthesis and characterisation of PCD coatings grown on Si wafer by the innovative 915 MHz microwave plasma chemical vapour deposition (MPCVD) technique.

Keywords: CVD diamond, polishing, characterisations, properties

1. Introduction

CVD grown diamond is an important class of material [1–6]. The characteristic of such material is very much dependant on the CVD processing conditions [7–21] and as well as on the post-processing steps that are equally significant for the efficient use of this material in engineering applications [22–26]. There are environments where it is exposed to heat under extreme conditions or it is rubbed against hard ceramic surfaces. Diamond is the hardest known material with very low coefficient of friction which naturally makes it a suitable tribological surface [27–29].

But the as grown diamond surface is very rough in nature which is required to be planarised before putting into real environments. It is well understood nowadays that the diamond nucleation and growth takes place first by coalescence of the seeded layer on the substrate surface and then on top of which diamond crystals grown in columnar fashion. Such vertical growth of crystals causes the top surface to be very rough and simultaneously there may be some inherent porosity present due to rise of such vertical columns. On the other hand, the nucleation side of the

freestanding diamond may have some porosity due to random coalescence of the islands during CVD processing. There is no such report of studying the surface area and porosity of CVD grown polycrystalline diamond (PCD). Here, it has been attempted for the first time to evaluate the pore size that may be present in the diamond coatings grown by CVD, using Brunauer-Emmett-Teller (BET) technique.

Moreover, tribological action may cause rise of temperature under humid atmospheric condition for diamond material to degrade. So it is necessary for the CVD grown diamond to be well characterised for the wear and friction applications [30–34]. Thermal stability has been studied so far by many authors [35–37] but it lacks proper assessment of oxidation temperature [38–40] since only standard furnaces have been used so far. Here, thermo-gravimetric analysis (TGA) and differential scanning calorimeter (DSC) techniques have been used for the first time ever to pinpoint the augmentation of oxidation.

Methane or other precursor gas compositions [41–45] determine the defects present inside the diamond crystals. For example, high methane concentration may cause many CVD growth defects which render the grown coating to become black/grey; whereas the cleaner processing conditions of low methane percentages etc. may cause the diamond coating to be white or transparent. Similarly boron or nitrogen in the precursor gases [46] make the diamond blue [47] or yellow [48–50] in colour due to the substitutional atomic defects [51, 52] introduced in the diamond lattice [53, 54]. Such substitutional defects are studied by [55] photoluminescence (PL) [56–58], Fourier transform infra-red (FTIR) spectroscopy techniques [59], whereas the point, line, plane or volume defects during CVD growth can be viewed under transmission electron microscopes (TEM) [60–68]. Post-processing steps such as annealing [69, 70] may be required to remove some of these defects [71]. Annealing [72–76] also makes the diamond to become purer in respect of graphitic inclusions. Raman spectra [77–79] reveal the phase purity of CVD grown diamonds [80–86]. Polishing is routinely done to reduce as-grown diamond surface roughness [87]. Tribology of such polished surfaces has been studied in detail but there is lack of literature [88–90] against silicon nitride ceramics [91] under machine oil lubrication [92]. Moreover, due to very hard and rough top surface of CVD grown PCD, researchers are hesitant to probe the as-grown PCD surface with their expensive Berkovich or other indenters [93–95]. In effect, there is not much literature [96–100] available which describes the mechanical properties [101, 102] of CVD grown PCDs.

Characterisation [103–107] of the CVD grown PCDs is very essential besides its synthesis. Some techniques which are frequently used for powder samples like, BET surface area analysis, TGA-DSC, Zetasizer particle size measurements are being reported here for the first time, for CVD polycrystalline diamond coatings. Moreover, black and white grades of diamond have been grown [108–110] and characterised so far, but their corresponding growth defects have not frequently been reported [111–113]. Here, authors have tried to elucidate the CVD growth defects that are present in their CVD grown diamonds. Afterwards, the PCD samples were polished to make them effective for tribological applications. Later on, such polished diamond surfaces have been mechanically characterised for studying tribological action [114] against silicon nitride balls under machine oil lubricants for the first time.

2. Materials and methods

2.1 Processing of polycrystalline diamond (PCD)

Polycrystalline diamond samples were fabricated with CSIR-CGCRI based DT1800 microwave plasma enhanced CVD (MPCVD) reactor on single crystal Si

wafers [115]. Deposition was carried out for 4–10 days to grow 0.5–0.8 mm thick diamond coatings. Reactor pressure and temperature were maintained in between 110 and 120 Torr and 900–1100°C, respectively. 1–3% methane in hydrogen gas mixture was used for growing diamond coatings with 9 kW input microwave power. Afterwards, PCDs were made freestanding by wet chemical etching of Si wafers with 1:1:1 ratio solution of $HF:HNO_3:CH_3COOH$ [116]. Such freestanding diamond wafers were cut in 6 mm diameter smaller discs by laser cutter (Hallmark Plus model. Nd-YAG lamp pumped laser with 10 watt power at 1064 nm wavelength). The diamond sample was then hot mounted to polish the as-grown rough surface [117]. Mechanical polishing was done using Leco, Germany polisher and subsequently CP4 model, Bruker, USA machine was used for chemo-mechanical polishing of the PCD samples. Metal bonded diamond disc and Cu-bonded diamond discs were used with different grit sizes for mechanical polishing with water as cooling agent. On the other hand, the chemo-mechanical polishing of diamond samples was carried out against alumina ceramic disc using $K_2S_2O_8$ solution and concentrated sulphuric acid along with diamond pastes. Separately, annealing of few diamond samples was also done at 600°C for 1 h in standard air furnace.

2.2 Physical characterisations of PCDs

The detonation nanodiamond (DND) particle size of the seeding slurry was measured by Malvern make Zetasizer instrument. Brunauer-Emmett-Teller (BET) surface area analyser (Quantachrome Instruments) was used to measure the surface area; and nitrogen adsorption isotherm (Barrett-Joyner-Halenda or BJH method) was used to measure the pore size and volume in the freestanding diamond coatings. The samples were degassed under vacuum at 100°C for 1 h prior to measurement. Thermogravimetric (TGA) and differential scanning calorimetry (DSC) analysis of the freestanding diamond sample was done at a heating rate of 10°C min^{-1} on a simultaneous thermal analyser (STA 449F, Netzsch, Germany). X-ray diffractograms (XRD) were recorded in the 2θ range 30°–100° at a slow scanning rate of 1° min^{-1} by an X-ray diffractometer (Philips X'Pert, The Netherlands) with Cu Kα radiation (at 40 kV and 40 mA). Transmission electron microscopy (TEM-Tecnai G2 30ST, FEI Company, USA) was used to evaluate the defects present inside the diamond lattice. FTIR/FIR spectrophotometer (Model: Frontier IRL 1280119, Perkin Elmer) attached with reflectance measurement arrangement with incident and reflectance angles set at 22.5°, was used for studying opaque and translucent PCD samples. The photoluminescence (PL) studies including emission and excitation measurements were carried out on a fluorescence spectrophotometer (Model: Quantum Master, enhanced NIR, from Photon Technologies International) using a xenon arc lamp of 60 W as a pump source. Raman spectra were obtained using a STR500, Cornes Technologies, (formerly known as Seki Technotron) micro-Raman spectrometer, with excitation by argon ion (514.5 nm) laser. The resolution was about 1 cm^{-1} with 1200 grating size. In all the Raman experiments, the laser spot size was 1–2 μm and an exposure time of 20 s was used which was repeated thrice to acquire the Raman signals during each measurement.

2.3 Mechanical and tribological characterisations of PCDs

Polished surfaces of the PCD samples were seen under a ZEISS Supra 35 (Germany) field emission scanning electron microscope (FESEM) with EDAX attachment. Roughness of the PCD surfaces were evaluated by a contact profilometer (Talysurf PGI 2000S, Taylor Hobson). The nanohardness and Young's modulus were measured by nanoindentation technique applied to the plan section

of the CVD grown polycrystalline diamond polished and nucleation side surfaces. A typical load of 1000 mN was used for the nanoindentation experiments. A standard nanoindenter (Fischerscope H100XY$_P$, Fischer, Switzerland) was used for this purpose. The nanoindenter machine was operated according to the DIN 50359-1 standard. It offered a load range of 0.4–1000 mN. It was equipped with a Berkovich indenter. The indenter possessed a tip radius of 150 nm. The machine was used in ambient laboratory conditions (23 ± 4°C, 70 ± 5% relative humidity). The depth sensing resolution of the machine was 1 nm. The force-sensing resolution of the machine was 0.2 μN. The machine was calibrated with nanoindentation based independent evaluation of H ≈ 4.14 ± 0.1 GPa and E ≈ 84.6 ± 3.5 GPa of a BK7 Glass (Schott, Germany). This material was provided by the supplier as a standard reference block. A ball-on-disc tribometer assembly (NANOVEA) was used for highly accurate and repeatable wear friction testing in rotational modes. The counter-face was a Si_3N_4 ball which was attached to a load arm and the load arm was directly in contact with experimental PCD disc surface. 3 mm diameter Si_3N_4 ball was in circular motion with 5 N applied normal load against PCD surface using commercially available machine oil lubricant in ambient laboratory condition. The speed of the ball was 0.04 m/s. Optical microscope (Olympus BX 51, country) study was done after each tribological experiment to know the radius of worn out silicon nitride ball.

3. Results and discussion

3.1 Physical characterisations—DND seed particle size, PCD crystallinity, porosity, growth defects and thermal stability

Detonation nanodiamond (DND) suspension in dimethyl sulfoxide (DMSO) by 0.5 wt% is used as seeding slurry for CVD growth of polycrystalline diamond material [118]. Nucleation density determines the faster grain coalescence phenomenon during chemical vapour deposition. It has been observed that DND seeds are much superior in enhancing nucleation of diamond than conventional micron size grits for seeding diamond nuclei on the foreign substrates [119]. The particle size of seeds is thus important in determining nucleation efficiency. One commercially available DND in DMSO was used for seeding. Before using to make seeding suspension by mixing it with 3 parts of methanol, it was essential to know the exact particle size distribution of such suspensions. Dynamic light scattering (DLS), is a non-invasive, well-established technique for measuring the size and size distribution of molecules and particles. The Brownian motion of particles or molecules in suspension causes laser light to be scattered at different intensities. Analysis of these intensity fluctuations yields the velocity of the Brownian motion and hence the particle size using the Stokes-Einstein relationship. The DND seeding suspension was procured from a commercial supplier and it was being used from time to time over a period of 1 year. When the particle size was calculated from DLS technique using Malvern make Zetasizer, it was found that the original suspension has become agglomerated considerably. The fresh stock of commercial suspension came with 25–30 nm DND particle size on its label but to our surprise after one long year in the shelf, the suspension only has 7% with original size of 25.56 nm whereas, 93% of the DND particles agglomerated to give an average size of 123.4 nm, as shown in the following **Figure 1a**. But such agglomeration does not appear to hinder its seeding efficiency.

The as-grown surfaces of the PCD coatings are very rough in nature which is labelled in **Figure 1b**. Cross-sectional microscopy image reveals columnar

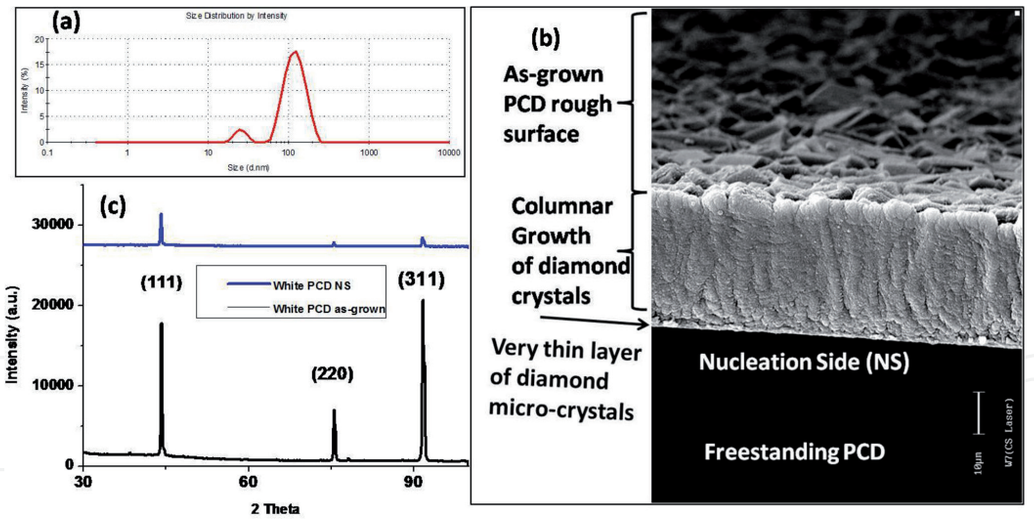

Figure 1.
(a) DND-DMSO seeding suspension particle size distribution; (b) cross-sectional SEM image of freestanding PCD; and (c) corresponding XRD signals from as-grown and nucleation side (NS).

growth of diamond crystals from the substrate side. The interface between the Si wafer and diamond columns consists of a very thin layer of diamond micro-crystals [116] which were initially coalesced with each other to form a continuous coating before diamond could grow vertically on top of them. Such thin crust layer on the nucleation side gives very poor XRD signals (top of **Figure 1c**) corresponding to diamond reflection planes, whereas, the peak intensities from the opposite as-grown surface (bottom one of **Figure 1c**) is very strong and characteristics of diamond cubic crystals. DND seeds initially formed islands which grow in a single layer until touching upon each other to form a continuous film. The diamond columns also do not grow exactly at 90° in the z direction. The adatoms from the plasma may add in a random way to produce some misorientation between the adjacent diamond columns. Moreover the top surface of diamond PCDs are very rough and sometimes appear porous. Such, (i) random coalescence of thin crust layer on the nucleation side, (ii) misorientation in between diamond columns and (iii) uneven as-grown surface of the diamond films, suggest that the CVD grown diamond may have some pores present in the freestanding coating. It is also true that in practice we assume that the CVD grown films are having 100% theoretical density but it is understood that that is not actually the case. So in order to know the pores that might present, BET surface area was calculated for the PCDs. Gas molecules are dosed into the sample chamber after cooling the solid down to a constant temperature in order to partially accumulate the gas molecules onto the solid surface which can be applied for the characterisation of surfaces as well as for the pore characterisation. The nitrogen adsorption at the temperature of liquid nitrogen (77 K) is standard method for such surface characterisation [120]. It is assumed that the nitrogen condenses onto the surface in a monolayer and so once the size of the gas atoms/molecules are known, the surface area can be estimated from the amount of adsorbed gas.

It was found that white PCD is having less surface area compare to the black PCD (**Table 1**). Nitrogen adsorption and desorption isotherms measured at 77 K allow the determination of pore volume and sizes. It was similarly observed that both the values are higher for black colour PCD. So it is inferred that black PCDs are having more CVD growth defects which is giving bigger pores and higher amount of porosity—i.e. addition of carbon atoms into the diamond sp3 lattice is more incoherent.

PCD sample	Surface area (m^2/g)	Pore volume (10^{-3} cc/g)	Pore diameter (nm)
White	1.19	1.82	3.51
Black	4.17	6.74	3.72

Table 1.
Freestanding PCD surface area and pore analysis.

PCDs grown using 3% CH_4 in H_2 resulted in black colour (**Figure 2a**), whereas, the coatings were white translucent in nature (**Figure 2b**) when 1% CH_4 was used. Colour of the freestanding diamond coatings vary due to the presence of defects inside the diamond lattice. For example when boron or nitrogen is substituting the carbon atoms, it results in blue or yellow colour of the diamond crystals. The PCD could become completely opaque or black in colour due to the presence growth defects like dislocations, twining, grain boundaries, stacking faults etc. [121]. **Figure 2c** and **2d** shows transmission electron microscopy images of the line defects pinned at grain boundary in one such poorer variety of black diamonds grown using 3% methane in hydrogen. On the other hand when 1% CH_4 was used to deposit diamond, the crystals were less defective and could synthesise white transparent freestanding coatings as shown in **Figure 2e**.

The quality of white PCD sample was found to be very high by Raman Spectroscopy. It has been found that under atmospheric conditions, the CVD diamond sample could sustain up to 700°C furnace temperature, but 750°C was not tolerable for the diamond material to resist oxidation. As per available literature [38], the procedure to study the thermal stability is to heat the diamond sample in an environment controlled furnace, but such procedure does not pinpoint the oxidation temperature of diamond material. In order to know the exact oxidation temperature of the CVD diamond prepared by DT1800 reactor, it was decided to conduct TGA-DSC experiments.

Figure 3 shows the TGA curve for white PCD sample when heated from room temperature at constant heating rate of 10 K/min in air with alumina crucible up

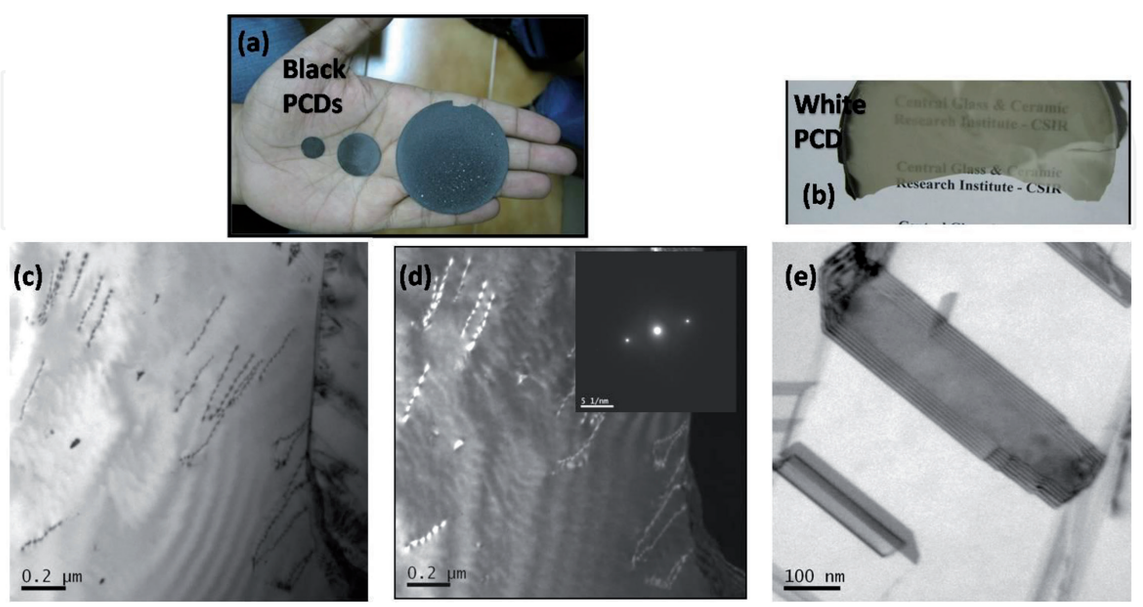

Figure 2.
(a) Black grade PCDs, (b) white grade PCD, (c) bright-field TEM image of a black PCD grain with some dislocations pinned at the grain boundary. (d) Corresponding wide beam dark field (WBDF) image showing clearly discernible dislocations. Inset shows the two-beam condition used for imaging the dislocations, (e) bright-field TEM image of defect free White PCD grain with some twins and grain—boundaries.

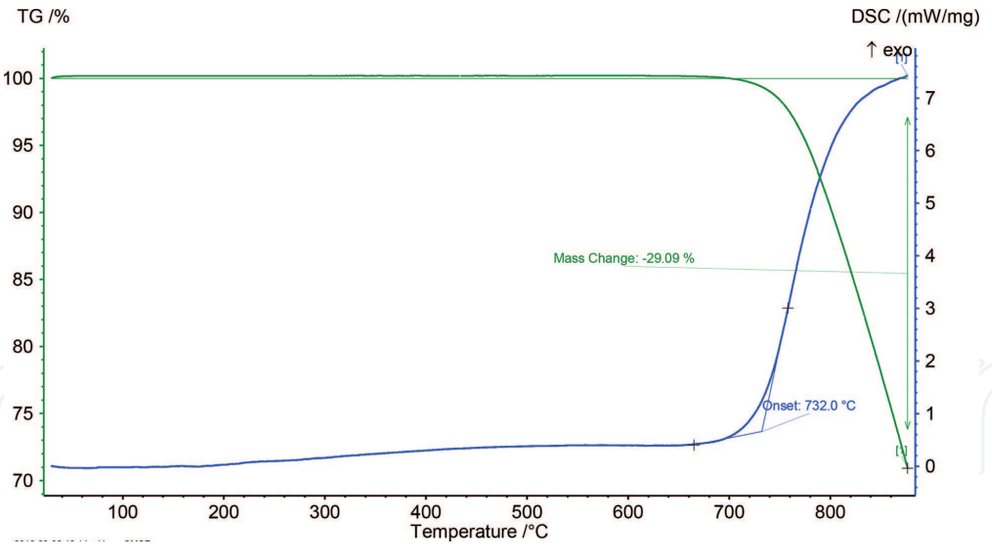

Figure 3.
TGA and DSC curves for heating CVD diamond in air.

to 900°C. There was no change in weight until 700°C temperature was crossed, after which there was continuous drop in weight, losing 29.09% of the initial value. The corresponding DSC curve shows that the exact onset temperature for oxidation reaction is 732°C, after drawing tangents. The weight loss can be attributed to the loss of carbon from diamond as gaseous by product of oxidation reaction. So, further to study the behaviour of CVD grown defects in PCD samples, they were heated in an air furnace at 600°C for 1 h. Such TGA-DSC curves confirm that annealed PCD samples do not undergo degradation on annealing and are good for studying the effect of heating on their internal defects.

3.2 Spectroscopy: FTIR, PL and Raman—PCD defects and annealing effects

3.2.1 FTIR studies

The FTIR reflectance spectra of as grown PCD samples, white PCD and black PCD, together with white PCD sample after being annealed at 600°C for 1 h are presented in **Figure 4**. The spectra reveal the presence of a broad absorption peak in the range 1745–2840 cm^{-1} in white PCD sample which may be attributed to the characteristic two phonon absorption of diamond [122, 123] and it is seen to be almost absent in black PCD sample. However, this peak disappears completely in annealed white PCD sample with simultaneous appearance of a new peak at 1090 cm^{-1}. Interestingly, the peak at 1090 cm^{-1} is observed to be more intense in as prepared black PCD sample. This peak marks the presence of N-defects in diamond lattice [123]. Thus, it can be stated that the as grown white PCD sample contains less nitrogen defects as compared to black PCD and is of better quality in terms of non-diamond inclusions. As a result characteristic carbon-carbon bond absorption vibrational modes are more distinct in white PCD as compared to black PCD, which has many internal planar and volume defects as already observed in **Figure 2**. But, annealing at 600°C results in the growth of atomic defect centres in white PCD sample. As the nitrogen impurity centres grow at the expense of carbon replacement in the lattice, intrinsic absorption band due to diamond is weakened while the vibrational band due to N-defects intensifies.

In addition, a third distinct peak is noticed at around 1490 cm^{-1} in both as grown white PCD and annealed sample which may be assigned to absorption due

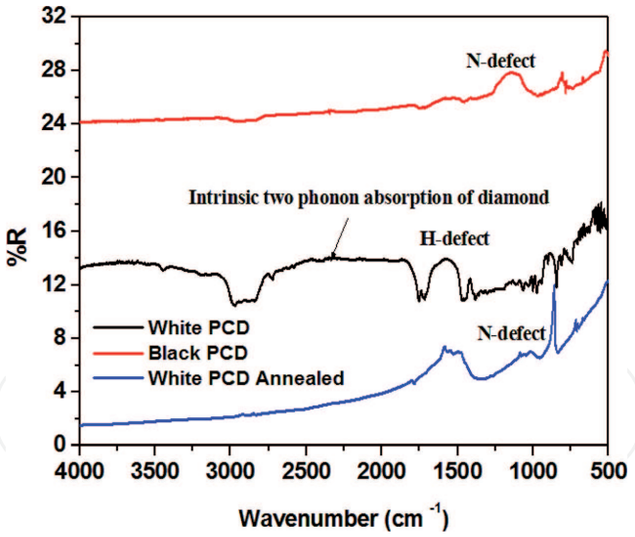

Figure 4.
FTIR spectra of different PCD samples.

to H-centres trapped in the lattice [124]. In black PCD sample this peak is seen to be extremely weak in nature. This may be explained on the basis of the processing condition of the two samples. White PCD was grown with 1% methane and 99% hydrogen whereas black PCD was grown with 3% methane and 97% hydrogen. Thus use of more hydrogen precursor during the CVD process may have resulted in trapping of H-centres in the lattice of white PCD. For further confirmation of the presence of impurity centres, photoluminescence study of these samples was performed.

3.2.2 Photoluminescence studies

Photoluminescence is a characteristic property of several defect centres in lattice and is thus a confirmatory tool for the presence of defects especially in diamonds. In an attempt to have detailed information regarding non-diamond inclusions, the photoluminescence spectra of all the samples were recorded under excitation of 270 nm wavelength and the spectra is presented in **Figure 5**.

The spectra reveal the presence of seven distinct peaks at 470, 496, 567, 625, 689, 734 and 767 nm respectively. Pezzagna et al. [125] suggests that small PL signal for neutral nitrogen vacancy centres is present at 575.67 nm, but for the negatively charged nitrogen vacancy centre, the PL peaks are observed at 637 nm with multiple phonon replica thereafter. It is also well known that silicon vacancy centre emits strong PL signal at 738 nm and a weak replica at 758 nm [121, 126]. Although nitrogen vacancy centres are best photo emitters for diamond but it has strong photon-phonon interactions which is responsible for broad emission spectrum from 600 to 850 nm. That may be the reason for us not getting the nitrogen vacancy signal exactly at the theoretical values in **Figure 5**. The peaks at the 567, 625 and 689 nm can be attributed to nitrogen vacancy centres, but not definitively. Similarly the peaks at 734 and 767 nm in **Figure 5** can be assigned to silicon vacancy centres but again, it is a complex defect centre with an impurity atom and vacancy—so the peaks are not always reproducible at identical positions. Surprisingly there are two more peaks in **Figure 5** at 470 and 496 nm which are typically found for Ni-related defect centres—but usually reported for HPHT synthetic diamonds [127]. It is not yet known about the origin of such PL peaks in CVD grown diamonds. Although the presence of the peaks can be identified in all the three samples, variation in the peak intensity indicates the difference in

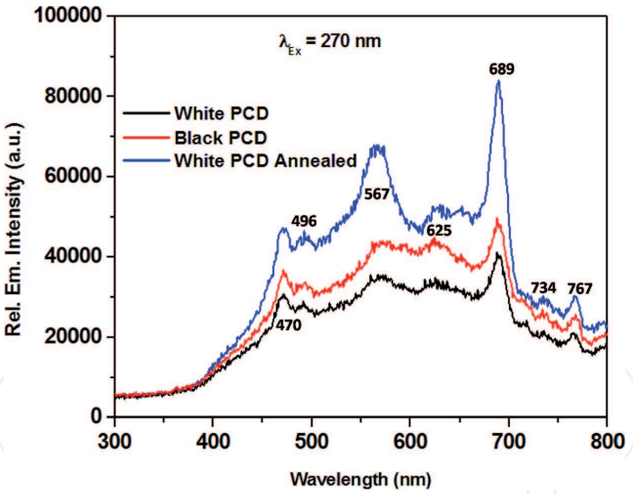

Figure 5.
Photoluminescence spectra of PCD samples.

quality of the samples. It is observed that black PCD sample exhibits the stronger peak intensity as compared to that of white PCD. This indicates white PCD contains lesser defect centres and is of better quality as compared to black PCD which is in accordance with the FTIR results. However, upon annealing white PCD sample is seen to exhibit strongest peak as compared to as prepared white PCD and black PCD samples. This signifies that the concentration of defects in white PCD is enhanced upon annealing which may be explained as due to possible aggregation of defect centres. At elevated temperature, the vacancy in a lattice becomes mobile and moves through the crystal and aggregates [128]. Vacancies upon encounter with isolated impurity atoms (nitrogen, silicon), forms the aggregation of defect centres thus resulting in enhanced luminescence.

3.2.3 Raman spectroscopy

The diamond peak positions of both the white and black annealed PCD samples are at 1328.45 cm^{-1} which is a downshift from the theoretical peak position for single crystal diamond as shown in **Figure 6**. Down shift of spectra is due to the tensile stress inside the lattice (thermal stress due to expansion mismatch with the Si substrate does not exist as the PCDs are freestanding) [129]. Now on the other hand, a-C (amorphous carbon) hump centre is around 1486 cm^{-1} for white annealed PCD but such diamond like carbon (DLC) phase centre shifts to 1560 cm^{-1} for the black annealed PCD sample. So this a-C hump central position change may be an indication of the nature of predominant amorphous carbon phase that is present in the samples. It is essentially trans-polyacetylene (TPA) for white annealed sample; whereas, the non-diamond carbon inside black annealed PCD is primarily graphitic carbon. The ratio of peak intensities of diamond to DLC gives estimation about the quality of the deposited diamond coating. Now to calculate the area under the curve, corresponding to the sp3 phase, the integration has been carried out from 1300 to 1360 cm^{-1}, which therefore would take into account of any upshift/downshift of the diamond peaks and disordered graphite that might also contaminate the coating. The integrated area for DLC phase is calculated from 1450 to 1600 cm^{-1}. As expected the quality of white annealed diamond (41%) has found to be better than the quality of the black annealed PCD (33%) sample. The FWHM value of diamond peak is also better for the white annealed PCD (4.62 cm^{-1}) than the black annealed PCD (7.38 cm^{-1}), as found from the analysis of the curves in **Figure 6**.

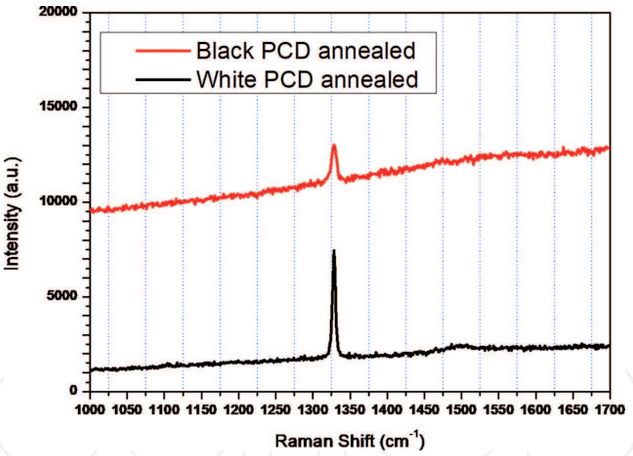

Figure 6.
Raman spectra of freestanding annealed PCD samples.

3.3 Mechanical characterisations: PCD polishing, nanoindentation and tribology

3.3.1 Polished PCD surfaces

Annealed samples were different from the PCD samples that were polished for mechanical property and tribology studies. Polishing was done to reduce the as grown surface roughness (**Figures 2b** and **7a**) which were in the order of 3–4 μm. Before starting polishing experiments, the white as grown PCDs were characterised by Raman spectroscopy (**Figure 7b**). It was found that the as-grown diamond samples were having tensile stress of about 0.8 GPa (calculated from the peak shift data). It also had some non-diamond impurity in the form of TPA which gives very little undulations around 1508 cm^{-1}. The FWHM was calculated to be 5.5 cm^{-1} at the diamond peak position. But when the Raman spectra were taken from the same white as-grown PCD sample after polishing, there is considerable enhancement of diamond peak intensity with appearance of graphitic D peak—giving shoulder to the sp3 peak position, centred around 1329 cm^{-1}. Tensile stress appears to increase on the surface of the same white PCD sample up to 1.34 GPa after polishing action. Moreover, the a-C hump becomes apparent in the polished sample which was not prominently present in the un-polished white PCD sample. The centre of a-C hump is around 1492 cm^{-1}, which indicates that the non-diamond composition was essentially trans-polyacetylene (TPA). FWHM of the diamond peak increases for the polished sample (7.65 cm^{-1}) which also confirms the degradation of the quality of the original (55%) white PCD surfaces after polishing (26%). **Figure 7c** shows the EDAX signals received from such polished surfaces under electron microscope. It can be seen that the carbon peak is not predominant due its low atomic weight. There are prominent peaks corresponding to metal elements like Fe, Bi, which might came from the metal bonded polishing discs. Moreover there are oxygen and sulphur elemental peaks also present, which are essentially from the oxidising chemicals used during chemo-mechanical polishing.

In order to reveal the morphology of polished diamond surfaces, **Figure 8** is provided with successive higher magnification images up to 25kX. It can be seen that there are longitudinal polishing marks, as shown by double headed arrows. Essentially the area under observation is covered with wear debris generated during both mechanical and chemo-mechanical polishing. Due to abrasive action of the polishing materials, fine particles were generated, which, when reacted with the polishing chemicals, were oxidised to dislodge diamond particles from

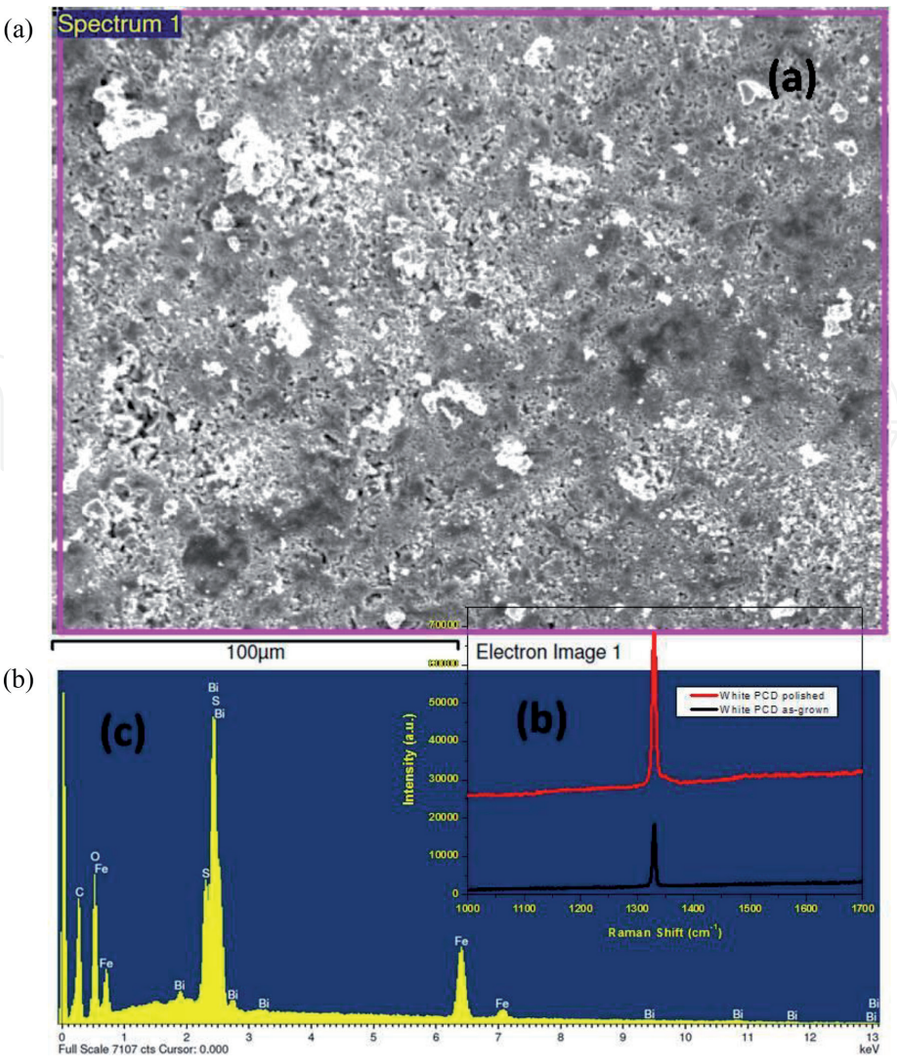

Figure 7.
(a) area scan of polished white PCD sample; (b) Raman spectra of as-grown and polished PCD samples; (c) EDAX signals from the scan area in (a) of the polished PCD sample.

the as-grown rough surfaces. Thus the final microstructures were like wear debris compressed under polishing load with intermediate pores and cracks. Some regions were very smooth with grooves present inside, whereas, their adjacent areas were very rough with scattered particles spread all over. It appears that such unclean top surface after polishing has to be annealed/chemically cleaned in order to remove non-diamond impurities and wear debris, before putting into use for technological application.

3.3.2 Hardness and elastic modulus

Nanoindentation was carried out on black and white PCD samples, both on the polished surfaces and on the mirror smooth nucleation sides (NS). Altogether four PCD surfaces were indented, as shown in **Figure 9**. The roughness of each surfaces are labelled in each **Figure 9**.

At least 10 nanoindentations were made along a line for the plan sections of each CVD grown polycrystalline diamond surfaces, at an applied load of 1000 mN. The time to reach the peak load was kept at 30 s for all the nanoindentation experiments. The unloading time was also kept same as the loading time. The experimental conditions for all the nanoindentation measurements were kept identical. From

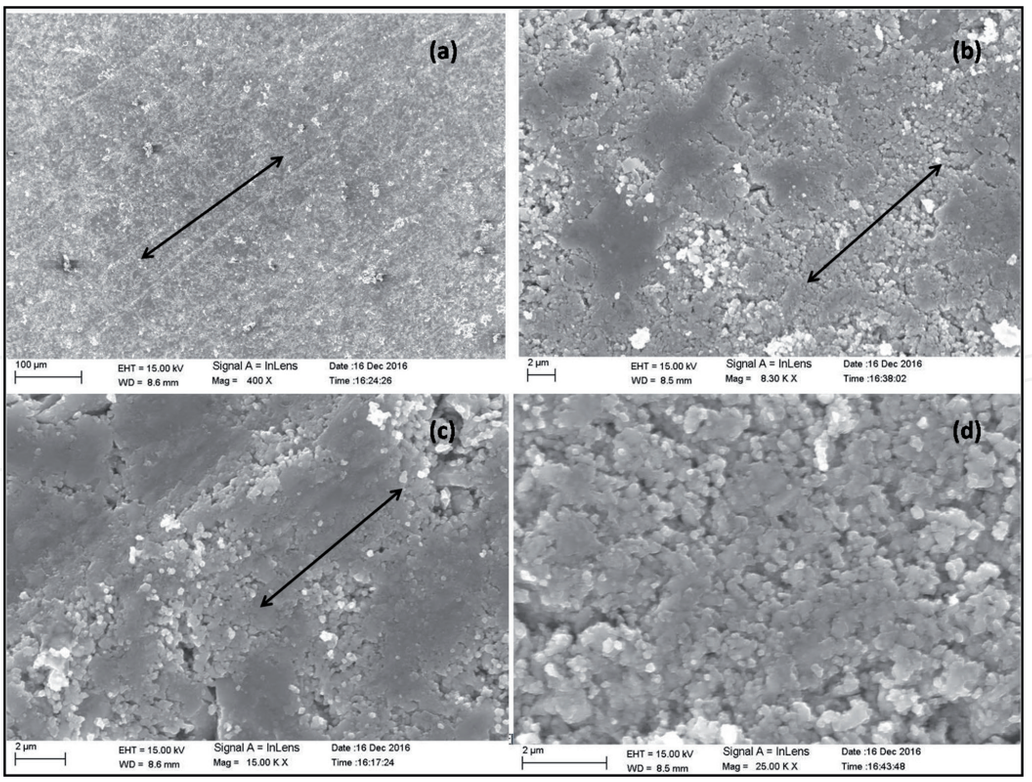

Figure 8.
SEM images of unclean polished white PCD sample at successive higher magnifications.

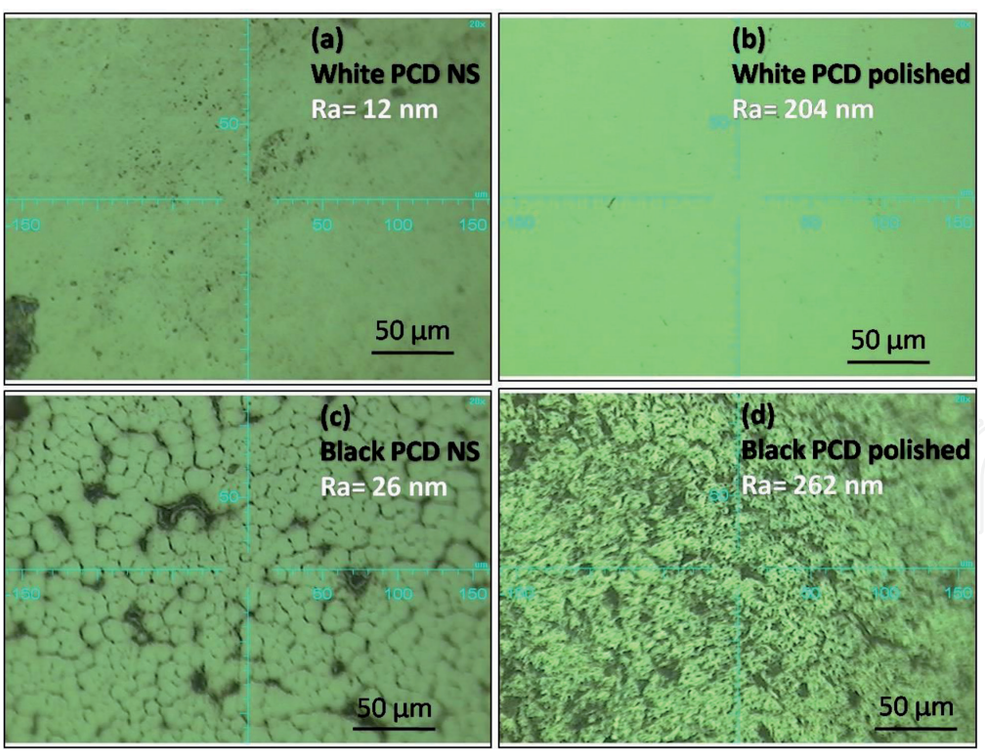

Figure 9.
Four different PCD surfaces probed with nanoindenter.

the experimentally measured load (P) versus depth of penetration (h) data, the nanohardness and Young's modulus values are evaluated for all PCD samples. Oliver and Pharr method [130] was utilised to evaluate the nanohardness and Young's modulus values.

The experimentally measured load (P) versus depth (h) plots for the plan sections of four different types of CVD grown polycrystalline diamond surface samples are shown

in **Figure 10**. In general, all the P-h plots were smooth in nature. An important observation from these data was that at comparable loads, the P-h plots of Black PCD NS, White PCD polished and Black PCD polished were much steeper than those of the White PCD NS sample. Moreover, at comparable loads the depth of penetration data recorded for the Black PCD NS, White PCD polished and Black PCD polished samples was much smaller than those of the White PCD NS sample. These data (**Figure 10**) indicated that nanohardness of Black PCD NS, White PCD polished and Black PCD polished would be higher than that of White PCD NS samples. The P-h plots obtained for White PCD NS samples showed more of the plastic deformation behaviour (**Figure 10**) compared to Black PCD NS, White PCD polished and Black PCD polished. However, the P-h plots obtained for Black PCD NS, White PCD polished and Black PCD polished samples showed more of the elasto-plastic deformation behaviour.

The nanohardness (H) of the PCD samples is shown in **Table 2**. Results show that the polished PCD surfaces have much higher hardness compare to their corresponding nucleation side, as expected. Black PCD has almost 5 GPa less hardness than white PCD polished surface, may be due to the presence of softer carbon phases other than diamond. But on the other hand, their corresponding nucleation sides are showing opposite trend—black PCD NS being harder than White PCD NS. It is already understood from our previous results and discussion that the black PCDs are having more CVD growth defects than white PCDs. Presence of such defects make the poorer variety diamond coatings black or grey in colour; their Raman signals become different as well as their other spectral data. **Figure 1b** and **c** shows that the as grown side is different from the nucleation side. Nucleation side has thin crust like layer whereas the as-grown side is having extended ends of the elongated diamond columnar crystals. From nanoindentation data, it is being revealed that the nucleation side of black quality diamond is harder which may be because of the presence of harder diamond like carbon phases than their white variety. Corresponding average Young's modulus (E) values showed the similar trend as nanohardness. The samples can be ranked in the increasing order of elastic modulus as follows: White PCD NS > Black PCD NS > Black PCD polished> White PCD polished. The hardness and elastic modulus results found in the present work are in agreement with the literature [93, 105] values.

3.3.3 Tribological properties

In order to understand the efficacy and necessity of the polishing method adopted in the present work, the white PCD sample was chosen for further

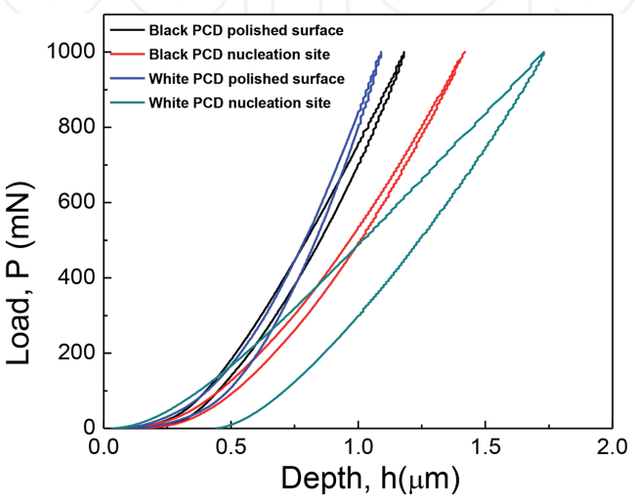

Figure 10.
Load vs. depth plots of nanoindentation PCD samples.

Samples	Hardness (GPa)	Young's modulus (GPa)
White PCD NS	10.82 ± 0.39	231.72 ± 8.24
White PCD polished	28.50 ± 2.78	1000.06 ± 157.61
Black PCD NS	14.71 ± 2.70	350.32 ± 84.79
Black PCD polished	23.17 ± 4.04	719.72 ± 189.07

Table 2.
Mechanical properties of PCD samples.

tribological studies. Both the polished and the corresponding opposite nucleation side were made to rotate against 3 mm diameter Si_3N_4 counter-face ball under machine oil lubrication. The coefficient of friction was found to be very low in compare to our earlier study of the similar polished/unpolished diamond surfaces against alumina balls [131]. Here also the diamond surfaces do not wear, but the counter body Si_3N_4 wears out, although not as severe as alumina ball which worn out under dry and SBF lubricating conditions by travelling half of the distance travelled by Si_3N_4 balls in the present case. The polished side of white PCD sample is rougher than their corresponding nucleation side (**Figure 9a** and **b**). So, as expected the COF values were found to be higher (~0.08) for polished white PCD surface than the nucleation side of white PCD sample (~0.03). The Hertzian contact pressure was calculated to be 26.2 GPa when 3 mm diameter ball was made to rotate against PCD disc surfaces under 5 N normal load as shown in schematic **Figure 11a**. The worn out ball was investigated under optical microscope (**Figure 12**) and the wear data was calculated as described in authors previous work [131]. It was found that the wear rate for the polished white PCD surface is very small 4.08×10^{-7} mm^3/N m and the wear rate for its corresponding nucleation side is much higher 3.95×10^{-5} mm^3/N m. The hardness of the polished side was found ~28 GPa, whereas its nucleation side was much softer with ~10 GPa nano-hardness. It is counter-intuitive that the counterbody Si_3N_4 wears out more against the softer diamond nucleation surface than while rubbing against the hard polished surface. In order to explain this apparent anomaly, it was necessary to know the hardness of Si_3N_4 from commercial supplier's database and it was found to be 10–12 GPa. Such comparable hardness values of diamond nucleation surface and Si_3N_4 counterbody might have caused nanodiamonds that are present in loosely held colonies [118] on the nucleation side to come out under abrasive wear action of silicon nitride. Such nanodiamonds that come out from the soft nucleation side under abrasive wear action may cause the Si_3N_4 counterbody to further wear out severely, since nanodiamonds are very hard particles.

CVD diamond surfaces sliding against silicon nitride balls reportedly give high COF values under dry lubricating conditions [91]. Researchers have tried commercial soybean-derived biodiesel lubricant [132] to improve the performance of the combustion engine. They could achieve 0.07 as the minimum value of COF when trying self-mated diamond coated Si_3N_4 material. They used 86 m of sliding distance under 2.5–4.5 GPa initial Hertzian contact pressures. Recently a graphene coating has also been applied on top of microcrystalline diamond surfaces to improve the COF values against Si_3N_4 balls under reciprocating actions [133]. 0.04 was the minimum achievable COF value. The researchers could notice wear track on such grapheme coated diamond flat surfaces. The calculated wear rate of the counterface Si_3N_4 ball from the measurement of the ball scar diameter was found to be in the order of 10^{-5} mm^3/N m. This same group of researchers also conducted a tribo-map of diamond films [134] against silicon nitride ceramics sliding in air, but under reciprocating action (present paper reports circular motion). The normal

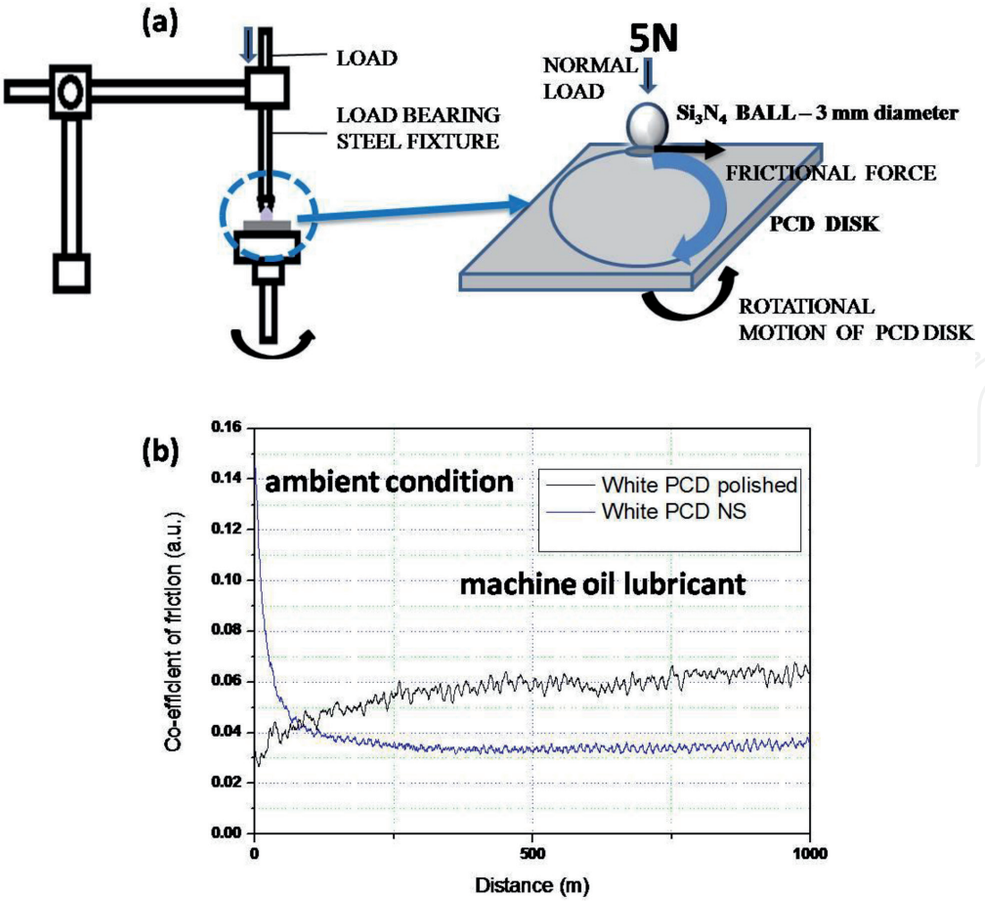

Figure 11.
(a) Schematic of ball-on-disc tribometer and (b) corresponding friction curves.

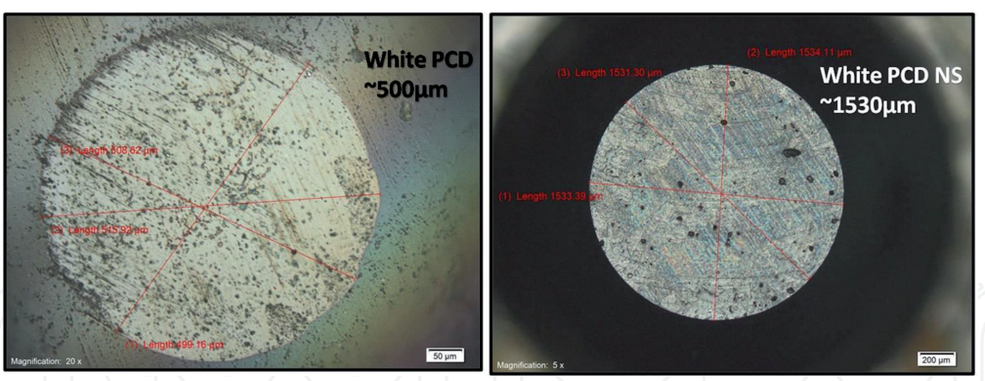

Figure 12.
Wear scar diameters on counterbody Si_3N_4 ball against white PCD (a) polished surface and (b) nucleation side surface.

load was 2–6 N, sliding speed was 0.13–0.3 m/s. They reported 0.07 as the best possible COF value with nanocrytsalline diamond, which was increased to 0.11, when the diamond film became microcrystalline. They also could observe worn out diamond film surface; and profilometer scan wear volume data revealed wear rate less than 10^{-7} mm^3/N m. Bogatov et al. [135] also reported >10^{-7} mm^3/N m wear rate of diamond film sliding against silicon nitride ball (ball characteristics were same as used in the present work) with 0.12 COF after 24,000 sliding cycles. But in the our present experiments with diamond disc, no wear track could be seen on the diamond disc surfaces sliding against silicon nitride balls—as also it was observed against alumina balls in authors' previous paper [131]. Only the balls worn out and the presented wear data of balls are in tandem with the reported literatures.

Moreover, the lowest COF of ~0.03 obtained using machine oil lubricant in the present paper appears to be better than liquid bio-diesel or solid grapheme lubricant used for diamond coatings previously.

4. Conclusions

As-grown, annealed, polished CVD grown diamonds have been characterised adopting some new techniques which are conventionally used for powder bulk specimens. Use of TGA-DSC analysis could pinpoint the diamond oxidation temperature for the first time. Attempt has been made to quantify the porosity that might be present in the freestanding coating, which reduces the theoretical density values of CVD grown diamond. It has been found that the internal defects that are present inside diamond lattice determine the black or white nature of diamond coatings. Qualitative analysis of such defects that are present in different grades of PCDs (line, plane or volume defects) like dislocations, grain boundary, twining has been revealed by transmission electron microscope. Whereas, the other atomic defects, like nitrogen vacancy, atomic hydrogen, are revealed by FTIR and PL studies. Raman signals quantify the internal stress, crystallinity and the quality of the CVD grown diamond coatings. It has been found that after polishing the surface of diamond becomes very unclean due to contamination from the polishing consumables and generation of non-diamond carbon phases. Use of machine oil lubricant for tribological application of such polished diamond surfaces has found to be very effective in reducing the COF values considerably. However, the CVD grown diamond nucleation side produced best COF value of about 0.03 with 3.95×10^{-5} $mm^3/N\ m$ wear rate for the silicon nitride counterface.

Acknowledgements

AKM is presently on Extraordinary Leave (EOL) from CSIR-CGCRI and working as FWO postdoctoral researcher at IMO-IMOMEC, University of Hasselt, Belgium. The work presented here was carried out during 1 year training programme on different instruments at the CSIR-CGCRI by the author. He acknowledges help in taking measurements and preparing the training report from research fellows and institute colleagues during his training programme, like Mr. Aniruddha Samanta, Ms. Debarati Ghosh, Ms. Snigdha Roy, to name a few, of the different divisions of CSIR-CGCRI.

Author details

Awadesh Kumar Mallik[1,2,3]

1 CSIR—Central Glass and Ceramic Research Institute, Kolkata, West Bengal, India

2 Institute for Materials Research (IMO), Hasselt University, Diepenbeek, Belgium

3 IMOMEC, IMEC vzw, Diepenbeek, Belgium

*Address all correspondence to: amallik@cgcri.res.in

References

[1] Gicquel A, Hassouni K, Silva F, Achard J. CVD diamond films: From growth to applications. Current Applied Physics. 2001;**1**:479-496. DOI: 10.1016/S1567-1739(01)00061-X

[2] Balmer RS, Brandon JR, Clewes SL, Dhillon HK, Dodson JM, Friel I, et al. Chemical vapour deposition synthetic diamond: Materials, technology and applications. Journal of Physics: Condensed Matter. 2009;**21**:364221. DOI: 10.1088/0953-8984/21/36/364221

[3] Nemanich RJ, Carlisle JA, Hirata A, Haenen K, guest editors. CVD diamond—Research, applications, and challenges. MRS Bulletin. 2014;**39**:490-494. DOI: 10.1557/mrs.2014.97

[4] Spear KE. Diamond-ceramic coating of the future. Journal of the American Ceramic Society. 1989;**72**:171-191

[5] May PW. Diamond thin films: A 21st-century material. Philosophical Transactions of the Royal Society of London. 2000;**358**:473-495

[6] Eaton-Magaña S, Shigley JE. Observations on CVD-grown synthetic diamonds: A review. Gems & Gemology. 2016;**52**:222-245

[7] Chernov VV, Gorbachev AM, Vikharev AL, Lobaev MA. Criterion for comparison of MPACVD reactors working at different microwave frequencies and diamond growth conditions. Physica Status Solidi A. 2016;**213**:2564-2569. DOI: 10.1002/pssa.201600193

[8] Teii K. Plasma deposition of diamond at low pressures: A review. IEEE Transactions on Plasma Science. 2014;**42**:3862-3869. DOI: 10.1109/TPS.2014.2333772

[9] Kasu M. Diamond epitaxy: Basics and applications. Progress in Crystal Growth and Characterization of Materials. 2016;**62**:317-328. DOI: 10.1016/j.pcrysgrow.2016.04.017

[10] Linnik SA, Gaydaychuk AV. Synthesis of multilayer polycrystalline diamond films using bias-induced secondary nucleation. Materials Letters. 2015;**139**:389-392. DOI: 10.1016/j.matlet.2014.10.142

[11] Schwander M, Partes K. A review of diamond synthesis by CVD processes. Diamond & Related Materials. 2011;**20**:1287-1301. DOI: 10.1016/j.diamond.2011.08.005

[12] Kromka A, Babchenko O, Izak T, Hruska K, Rezek B. Linear antenna microwave plasma CVD deposition of diamond films over large areas. Vacuum. 2012;**86**:776-779. DOI: 10.1016/j.vacuum.2011.07.008

[13] Nor RM, Bakar SA, Thandavan TM, Rusop M. Diamond: Synthesis, characterisation and applications, carbon and oxide nanostructures. Advanced Structured Materials. 2010;**5**:195-217

[14] Muchnikov AB, Vikharev AL, Radishev DB, Isaev VA, Ivanov OA, Gorbachev AM. A wafer of combined single-crystalline and polycrystalline CVD diamond. Materials Letters. 2015;**139**:1-3. DOI: 10.1016/j.matlet.2014.10.022

[15] Kar R, Patel NN, Chand N, Shilpa RK, Dusane RO, Patil DS, et al. Detailed investigation on the mechanism of co-deposition of different carbon nanostructures by microwave plasma CVD. Carbon. 2016;**106**:233-242. DOI: 10.1016/j.carbon.2016.05.027

[16] Goncalves JAN, Sandonato GM, Iha K. Characterization of boron doped CVD diamond films by Raman spectroscopy and X-ray diffractometry.

Diamond and Related Materials. 2002;**11**:1578-1583. DOI: 10.1016/S0925-9635(02)00103-6

[17] Fries MD, Vohra YK. Properties of nanocrystalline diamond thin films grown by MPCVD for biomedical implant purposes. Diamond and Related Materials. 2004;**13**:1740-1743. DOI: 10.1016/j.diamond.2004.02.014

[18] Palyanov YN, Kupriyanov IN, Khokhryakov AF, Ralchenko VG. Crystal Growth of Diamond, Handbook of Crystal Growth. Bulk Crystal Growth, A Volume in Handbook of Crystal Growth. 2nd ed. 2015. pp. 671-713. DOI: 10.1016/B978-0-444-63303-3.00017-1

[19] Terranova ML, Rossi M, Tamburri E. Nanocrystalline sp2 and sp3 carbons: CVD synthesis and applications. Crystallography Reports. 2016;**61**:897-906. DOI: 10.1134/S1063774516060158

[20] Bogatskiy A, Butler JE. A geometric model of growth for cubic crystals: Diamond. Diamond & Related Materials. 2015;**53**:58-65. DOI: 10.1016/j.diamond.2014.12.010

[21] Hua C, Yan X, Wei J, Guo J, Liu J, Chen L, et al. Intrinsic stress evolution during different growth stages of diamond film. Diamond & Related Materials. 2017;**73**:62-66. DOI: 10.1016/j.diamond.2016.12.008

[22] Lobanov SS, Prakapenka VB, Prescher C, Konopkov Z, Liermann HP, Crispin KL, et al. Pressure, stress, and strain distribution in the double-stage diamond anvil cell. Journal of Applied Physics. 2015;**118**:035905. DOI: 10.1063/1.4927213

[23] Nedosekin P, Gladchenkov E, Zakharchenko K, Kolyubin V. Review the space radiation CVD diamond multi-layer detector. Moscow: International Siberian Conference on Control and Communications (SIBCON). 2016. pp. 1-4. DOI: 10.1109/SIBCON.2016.7491780

[24] Cui Y, Wang W, Shen B, Sun F. Reprint of "A study of CVD diamond deposition on cemented carbide ball-end milling tools with high cobalt content using amorphous ceramic interlayers". Diamond & Related Materials. 2016;**63**:51-59. DOI: 10.1016/j.diamond.2016.01.017

[25] Shen B, Sun FH, Zhang ZM, Shen HS, Guo SS. Application of ultra-smooth composite diamond film coated WC–Co drawing dies under water-lubricating conditions. Transactions of Nonferrous Metals Society of China. 2013;**23**:161-169. DOI: 10.1016/S1003-6326(13)62443-7

[26] Shen B, Sun F. Deposition and friction properties of ultra-smooth composite diamond films on Co-cemented tungsten carbide substrates. Diamond and Related Materials. 2009;**18**:238-243. DOI: 10.1016/j.diamond.2008.10.053

[27] Dumpala R, Chandran M, Ramachandra Rao MS. Engineered CVD diamond coatings for machining and tribological applications. JOM. 2015;**67**:1565-1577. DOI: 10.1007/s11837-015-1428-2

[28] Tian Q, Yang B, Zhuang H, Guo Y, Wang C, Zhai Z, et al. Hybrid diamond/graphite films: Morphological evolution, microstructure and tribological properties. Diamond & Related Materials. 2016;**70**:179-185. DOI: 10.1016/j.diamond.2016.10.020

[29] Nagasaka H, Ito K, Mori J, Shimizu T, Sasaki S. Tribological properties of polycrystalline diamond films prepared by hot-filament chemical vapor deposition methods. In: Proceedings of the 16th International Conference on

Nanotechnology; August 22-25 2016; Sendai, Japan. 2016. pp. 616-619

[30] Shen B, Chen S, Sun F. Investigation on the long-duration tribological performance of bilayered diamond/diamond-like carbon films. Proceedings of the Institution of Mechanical Engineers, Part J: Journal of Engineering Tribology. 2014;**228**:628-641. DOI: 10.1177/1350650114522611

[31] Zhang D, Shen B, Sun F. Study on tribological behavior and cutting performance of CVD diamond and DLC films on Co-cemented tungsten carbide substrates. Applied Surface Science. 2010;**256**:2479-2489. DOI: 10.1016/j.apsusc.2009.10.092

[32] Xinchang W, Liang W, Bin S, Fanghong S. Friction and wear performance of boron doped, Undoped microcrystalline and fine grained composite diamond films. Chinese Journal of Mechanical Engineering. 2015;**28**:155-163. DOI: 10.3901/CJME.2014.1114.168

[33] Chen N, Pu L, Sun F, He P, Zhu Q, Ren J. Tribological behavior of HFCVD multilayer diamond film on silicon carbide. Surface & Coatings Technology. 2015;**272**:66-71. DOI: 10.1016/j.surfcoat.2015.04.023

[34] Jones AN, Ahmed W, Rego CA, Taylor H, Beake BD, Jackson MJ. Investigation of the tribological properties of diamond films. Journal of Materials Engineering and Performance. 2007;**16**:131-134. DOI: 10.1007/s11665-006-9021-z

[35] Kumaran CR, Tiwari B, Chandran M, Bhattacharya SS, Ramachandra Rao MS. Effect of temperature on the stability of diamond particles and continuous thin films by Raman imaging. Journal of Nanoparticle Research. 2013;**15**:1509

[36] Ren B, Huang J, Yu H, Yang W, Wang L, Pan Z, et al. Thermal stability of hydrogenated diamond films in nitrogen ambience studied by reflection electron energy spectroscopy and X-ray photoelectron spectroscopy. Applied Surface Science. 2016;**388**:565-570. DOI: 10.1016/j.apsusc.2015.10.067

[37] Nakazawa H, Okuno S, Magara K, Nakamura K, Miura S, Enta Y. Tribological properties and thermal stability of hydrogenated, silicon/nitrogen-coincorporated diamond-like carbon films prepared by plasma-enhanced chemical vapor deposition. Japanese Journal of Applied Physics. 2016;**55**:12550. DOI: 10.7567/JJAP.55.125501

[38] Zolotukhin A, Kopylov PG, Ismagilov RR, Obraztsov AN. Thermal oxidation of CVD diamond. Diamond & Related Materials. 2010;**19**:1007-1011. DOI: 10.1016/j.diamond.2010.03.005

[39] Fecher J, Wormser M, Rosiwal SM. Long term oxidation behavior of micro- and nano-crystalline CVD diamond foils. Diamond & Related Materials. 2016;**61**:41-45. DOI: 10.1016/j.diamond.2015.11.009

[40] Lee J, Anderson MW, Gray FA, John P, Lee J, Baik Y, et al. Oxidation of CVD diamond powders. Diamond and Related Materials. 2004;**13**:1070-1074. DOI: 10.1016/j.diamond.2004.01.026

[41] Joung YH, Kang FS, Lee S, Kang H, Choi WS, Choi YK, et al. Reaction gas ratio effect on the growth of a diamond film using microwave plasma-enhanced chemical vapor deposition. Journal of Nanoscience and Nanotechnology. 2016;**16**:5295-5297. DOI: 10.1166/jnn.2016.12212

[42] Lloret F, Araujo D, Eon D, Villar MP, Gonzalez-Leal JM, Bustarret E. Influence of methane concentration on MPCVD overgrowth of 100-oriented etched diamond substrates. Physica Status Solidi A. 2016;**213**:2570-2574. DOI: 10.1002/pssa.201600182

[43] Izak T, Davydova M, Varga M, Potocky S, Kromka A. Growth rate enhancement and morphology engineering of diamond films by adding CO_2 or N_2 in hydrogen rich gas chemistry. Advanced Science, Engineering and Medicine. 2014;**6**:749-755. DOI: 10.1166/asem.2014.1571

[44] Yang L, Jiang C, Guo S, Zhang L, Gao J, Peng J, et al. Novel diamond films synthesis strategy: Methanol and argon atmosphere by microwave plasma CVD method without hydrogen. Nanoscale Research Letters. 2016;**11**:415. DOI: 10.1186/s11671-016-1628-x

[45] Liu C, Wang JH, Weng J. Growth of micro-and nanocrystalline dual layer composite diamond films by microwave plasma CVD: Influence of CO_2 concentration on growth of nano-layer. Journal of Crystal Growth. 2015;**410**:30-34. DOI: 10.1016/j.jcrysgro.2014.10.040

[46] Paxton WF, Howell M, Kang WP, Davidson JL. Influence of hydrogen on the thermionic electron emission from nitrogen-incorporated polycrystalline diamond films. Journal of Vacuum Science & Technology B. 2012;**30**:021202. DOI: 10.1116/1.3684982

[47] Zou Y, Larsson K. Effect of boron doping on the CVD growth rate of diamond. Journal of Physical Chemistry C. 2016;**120**:10658-10666. DOI: 10.1021/acs.jpcc.6b02227

[48] Lobaev MA, Gorbachev AM, Bogdanov SA, Vikharev AL, Radishev DB, Isaev VA, et al. Influence of CVD diamond growth conditions on nitrogen incorporation. Diamond & Related Materials. 2017;**72**:1-6. DOI: 10.1016/j.diamond.2016.12.011

[49] Zaitsev AM, Wang W, Moe KS, Johnson P. Spectroscopic studies of yellow nitrogen-doped CVD diamonds. Diamond & Related Materials. 2016;**68**:51-61. DOI: 10.1016/j.diamond.2016.06.002

[50] Ficek M, Sankaran KJ, Ryl J, Bogdanowicz R, Lin I, Haenen K, et al. Ellipsometric investigation of nitrogen doped diamond thin films grown in microwave $CH_4/H_2/N_2$ plasma enhanced chemical vapor deposition. Applied Physics Letters. 2016;**108**:241906. DOI: 10.1063/1.4953779

[51] Kono S, Teraji T, Kodama H, Sawabe A. Reprint of "imaging of diamond defect sites by electron-beam-induced current". Diamond & Related Materials. 2016;**63**:30-37. DOI: 10.1016/j.diamond.2016.01.020

[52] Khan RUA, Cann BL, Martineau PM, Samartseva J, Freeth JJP, Sibley SJ, et al. Colour-causing defects and their related optoelectronic transitions in single crystal CVD diamond. Journal of Physics: Condensed Matter. 2013;**25**:275801. DOI: 10.1088/0953-8984/25/27/275801

[53] Prokhorova IA, Voloshinb AE, Ralchenko VG, Bolshakov AP, Romanove DA, Khomich AA, et al. X-ray diffraction characterization of epitaxial CVD diamond films with natural and isotopically modified compositions. Crystallography Reports. 2016;**61**:979-986. DOI: 10.1134/S1063774516060122

[54] Chowdhury S, Laugier MT, Henry J. XRD stress analysis of CVD diamond coatings on SiC substrates. International Journal of Refractory Metals & Hard Materials. 2007;**25**:39-45. DOI: 10.1016/j.ijrmhm.2005.11.012

[55] Willems B, Tallaire A, Achard J. Optical study of defects in thick undoped CVD synthetic diamond layers. Diamond & Related Materials. 2014;**41**:25-33. DOI: 10.1016/j.diamond.2013.09.010

[56] Collins AT. The characterisation of point defects in diamond by luminescence spectroscopy. Diamond

and Related Materials. 1992;**1**:457-469. DOI: 10.1016/0925-9635(92)90146-F

[57] Zaitsev AM, Moe KS, Wang W. Optical centers and their depth distribution in electron irradiated CVD diamond. Diamond & Related Materials. 2017;**71**:38-52. DOI: 10.1016/j.diamond.2016.11.015

[58] Ralchenko V, Sedov V, Saraykin V, Bolshakov A, Zavedeev E, Ashkinazi E, et al. Precise control of photoluminescence of silicon-vacancy color centers in homoepitaxial single-crystal diamond: Evaluation of efficiency of Si doping from gas phase. Applied Physics A: Materials Science & Processing. 2016;**122**:795. DOI: 10.1007/s00339-016-0343-x

[59] Walker J. Optical absorption and luminescence in diamond. Reports on Progress in Physics. 1979;**42**:1606-1659. DOI: 10.1088/0034-4885/42/10/001

[60] Sawada H, Ichinose H. Atomic structure of fivefold twin center in diamond film. Diamond & Related Materials. 2005;**14**:109-112. DOI: 10.1016/j.diamond.2004.07.016

[61] Purwanto S, Iskandar R, Dimyati A. Scanning transmission electron microscopy (STEM) study on surface modified CVD diamond/Si(111) film post implanted Fe-B and NiFe-B related to GMR properties. AIP Conference Proceedings. 2016;**1725**:020064. DOI: 10.1063/1.4945518

[62] Ma GHM, Lee YH, Glass JT. Electron microscopic characterization of diamond films grown on Si by bias-controlled chemical vapor deposition. Journal of Materials Research. 1990;**5**:2367-2377. DOI: 10.1557/JMR.1990.2367

[63] Quin LC, Zhou D, Krauss AR, Gruen DM. TEM characterisation of nanodiamond thin films. Nanostructured Materials. 1998;**10**:649-660. DOI: 10.1016/S0965-9773(98)00092-0

[64] Nistor LC, Landuyt JV, Ralchenko VG, Obraztsova ED, Smolin AA. Nanocrystalline diamond films: Transmission electron microscopy and Raman spectroscopy characterisation. Diamond and Related Materials. 1997;**6**:159-168. DOI: 10.1016/S0925-9635(96)00743-1

[65] Pal KS, Bysakh S, Mallik AK, Dandapat N, Datta S, Guha BK. Influence of growth conditions on microstructure and defects in diamond coatings grown by microwave plasma enhanced CVD. Bulletin of Materials Science. 2015;**38**:1-8 http://www.ias.ac.in/article/fulltext/boms/038/03/0717-0724

[66] Berger D, Uhlmann E, Dethlefs I. A novel method for specimen preparation and analysis of CVD diamond coated tools using focussed ion beams (FIB) and scanning electron microscopy (SEM). Metallography, Microstructure, and Analysis. 2015;**4**:49-57. DOI: 10.1007/s13632-014-0184-y

[67] Sawada H, Ichinose H, Kohyama M. Atomic structure of the R3 and R9 grain boundaries in CVD diamond film. Scripta Materialia. 2004;**51**:689-692. DOI: 10.1016/j.scriptamat.2004.06.011

[68] Porro S, Temmerman GD, MacLaren DA, Lisgo S, Rudakov DL, Westerhout J, et al. Surface analysis of CVD diamond exposed to fusion plasma. Diamond & Related Materials. 2010;**19**:818-823. DOI: 10.1016/j.diamond.2010.01.051

[69] Zhang M, Xia Y, Wang L, Gu B, Su Q, Lou Y. Effects of the deposition conditions and annealing process on the electric properties of hot-filament CVD diamond films. Journal of Crystal Growth. 2005;**274**:21-27. DOI: 10.1016/j.jcrysgro.2004.09.092

[70] Yan X, Wei J, Guo J, Hua C, Liu J, Chen L, et al. Mechanism of graphitization and optical degradation of CVD diamond films by rapid heating treatment. Diamond and Related Materials. 2017;**73**:39-46. DOI: 10.1016/j.diamond.2016.11.010

[71] Khomich AA, Kudryavtsev OS, Dolenko TA, Shiryaev AA, Fisenko AV, Konov VI, et al. Anomalous enhancement of nanodiamond luminescence upon heating. Laser Physics Letters. 2017;**14**:025702. DOI: 10.1088/1612-202X/aa52f5

[72] Khomich A, Ralchenko VG, Nistor L, Vlasov I, Khmelnitskiy R. Optical properties and defect structure of CVD diamond films annealed at 900-1600°C. Physica Status Solidi (a). 2000;**181**:37-44. DOI: 10.1002/1521-396X(200009)181:1<37::AID-PSSA37>3.0.CO;2-T

[73] Yamamoto T, Umeda T, Watanabe K, Onoda S, Markham ML, Twitchen DJ, et al. Extending spin coherence times of diamond qubits by high temperature annealing. Physical Review B. 2013;**88**:075206. DOI: https://doi.org/10.1103/PhysRevB.88.075206

[74] Khomich AV, Ralchenko VG, Vlasov AV, Khmelnitskiy RA, Vlasov II, Konov VI. Effect of high temperature annealing on optical and thermal properties of CVD diamond. Diamond and Related Materials. 2001;**10**:546-551. DOI: 10.1016/S0925-9635(00)00517-3

[75] Ralchenko VG, Nistor L, Pleuler E, Khomich A, Vlasov I, Khmelnitskiy R. Structure and properties of high-temperature annealed CVD diamond. Diamond and Related Materials. 2003;**12**:1964-1970. DOI: 10.1016/S0925-9635(03)00214-0

[76] Seshan V, Ullien D, Castellanos-Gomez A, Sachdeva S, Murthy DHK, Savenije TJ, et al. Hydrogen termination of CVD diamond films by high-temperature annealing at atmospheric pressure. The Journal of Chemical Physics. 2013;**138**:234707. DOI: 10.1063/1.4810866

[77] Dychalska A, Fabisiak K, Paprocki K, Makowiecki J, Iskaliyeva A, Szybowicz M. A Raman spectroscopy study of the effect of thermal treatment on structural and photo luminescence properties of CVD diamond films. Materials and Design. 2016;**112**:320-327. DOI: 10.1016/j.matdes.2016.09.092

[78] Sanzenbacher LM. Raman Spectroscopic Studies of Single Crystal Diamond [MS Thesis]. Graduate Program in Chemical Physics The Ohio State University; 2011. pp. 1-41

[79] Ferrari AC, Robertson J. Raman spectroscopy of amorphous, nanostructured, diamond-like carbon, and nanodiamond. Philosophical Transactions of the Royal Society of London. Series A. 2004;**362**:2477-2512. DOI: 10.1098/rsta.2004.1452

[80] Haubnera R, Rudigiera M. Raman characterisation of diamond coatings using different laser wavelengths. Physics Procedia. 2013;**46**:71-78. DOI: 10.1016/j.phpro.2013.07.047

[81] Prawer S, Nemanich RJ. Raman spectroscopy of diamond and doped diamond. Philosophical Transactions of the Royal Society of London. Series A. 2004;**362**:2537-2565. DOI: 10.1098/rsta.2004.1451

[82] Knight DS, White WB. Characterization of diamond films by Raman spectroscopy. Journal of Materials Research. 1989;**4**:385-393. DOI: 10.1557/JMR.1989.0385

[83] Pandey M, D'Cunha R, Tyagi AK. Defects in CVD diamond: Raman and XRD studies. Journal of Alloys and Compounds. 2002;**333**:260-265. DOI: 10.1016/S0925-8388(01)01740-6

[84] Bachmann PK, Bausen HD, Lade H, Leers D, Wiechert DU, Herres N, et al. Raman and X-ray studies of polycrystalline CVD diamond films. Diamond and Related Materials. 1994;**3**:1308-1314. DOI: 10.1016/0925-9635(94)901430

[85] Solin SA, Ramdas AK. Raman spectrum of diamond. Physical Review B. 1970;**1**:1687, 1698. DOI: 10.1103/PhysRevB.1.1687

[86] Filik J. Raman spectroscopy: A simple, non-destructive way to characterize diamond and diamond-like carbon materials. Spectroscopy Europe. 2005;**17**:1010-1017

[87] Chen N, Ai J, Chen Y, He P, Ren J, Ji D. Multilayer strategy and mechanical grinding for smoothing CVD diamond coated defective substrate. Materials and Design. 2016;**103**:194-200. DOI: 10.1016/j.matdes.2016.04.069

[88] Kellermann K, Ehrhardt S, Fandrey J, Rosiwal SM, Singer RF. Influence of surface roughness on the tribological properties of HF-CVD diamond coated heat-treatable steel. Wear. 2010;**269**:811-815. DOI: 10.1016/j.wear.2010.08.009

[89] Schade A, Rosiwal SM, Singer RF. Influence of surface topography of HF-CVD diamond films on self-mated planar sliding contacts in dry environments. Surface & Coatings Technology. 2007;**201**:6197-6205. DOI: 10.1016/j.surfcoat.2006.11.024

[90] Zhang R, Lub Z, Shi W, Leng S, Tang B. Low friction of diamond sliding against Al2O3 ceramic ball based on the first principles calculations. Surface & Coatings Technology. 2015;**283**:129-134. DOI: 10.1016/j.surfcoat.2015.10.062

[91] Wang X, Shen X, Zhao T, Sun F, Shen B. Tribological properties of SiC-based MCD films synthesized using different carbon sources when sliding against Si_3N_4. Applied Surface Science. 2016;**369**:448-459. DOI: 10.1016/j.apsusc.2016.01.249

[92] Miyake S, Shindo T, Miyake M. Friction properties of surface-modified polished chemical-vapor-deposited diamond films under boundary lubrication with water and poly-alpha olefin. Tribology International. 2016;**102**:287-296. DOI: 10.1016/j.triboint.2016.05.026

[93] Fazio LD, Syngellakis S, Wood RJK, Fugiuele FM, Sciume G. Nanoindentation of CVD diamond: Comparison of an FE model with analytical and experimental data. Diamond and Related Materials. 2001;**10**:765-769. DOI: 10.1016/S0925-9635(00)00496-9

[94] Nitti MA, Cicala G, Brescia R, Romeo A, Guion JB, Perna G, et al. Mechanical properties of MWPECVD diamond coatings on Si substrate via nanoindentation. Diamond & Related Materials. 2011;**20**:221-226. DOI: 10.1016/j.diamond.2010.12.002

[95] Chowdhury S, de Barra E, Laugier MT. Hardness measurement of CVD diamond coatings on SiC substrates. Surface Coatings & Technology. 2005;**193**:200-205. DOI: 10.1016/j.surfcoat.2004.08.131

[96] Mohr M, Picollo F, Battiato A, Bernardi E, Forneris J, Tengattini A, et al. Characterization of the recovery of mechanical properties of ion-implanted diamond after thermal annealing. Diamond & Related Materials. 2015;**63**:75-79. DOI: 10.1016/j.diamond.2015.11.008

[97] Wiora M, Bruehne K, Floeter A, Gluche P, Willey TM, Kucheyev SO, et al. Grain size dependent mechanical properties of nanocrystalline diamond films grown by hot-filament CVD. Diamond & Related Materials.

2009;**18**:927-930. DOI: 10.1016/j.diamond.2008.11.026

[98] Cicala G, Magaletti V, Senesi GS, Carbone G, Altamura D, Giannini C, et al. Superior hardness and Young's modulus of low temperature nanocrystalline diamond coatings. Materials Chemistry and Physics. 2014;**144**:505-511. DOI: 10.1016/j.matchemphys.2014.01.027

[99] Hei LF, Lu FX, Li CM, Tang WZ, Chen GC, Song JH. A review on mechanical properties of freestanding diamond films. Advanced Materials Research. 2012;**490-495**:3059-3064. DOI: 10.4028/www.scientific.net/AMR.490-495.3059

[100] Kamiya S, Takahashi H, Kobayashi A, Saka M, Abe H. Fracture strength of chemically vapor deposited diamond on the substrate and its relation to the crystalline structure. Diamond and Related Materials. 2000;**9**:1110-1114. DOI: 10.1016/S0925-9635(99)00331-3

[101] Kulisch W, Popov C, Boychev S, Buforn L, Favaro G, Conte N. Mechanical properties of nanocrystalline diamond/amorphous carbon composite films prepared by microwave plasma chemical vapour deposition. Diamond & Related Materials. 2004;**13**:1997-2002. DOI: 10.1016/j.diamond.2004.04.002

[102] Wang X, Shen X, Sun F, Shen B. Mechanical properties and solid particle erosion of MCD films synthesized using different carbon sources by BE-HFCVD. International Journal of Refractory Metals and Hard Materials. 2016;**54**:370-377. DOI: 10.1016/j.ijrmhm.2015.09.004

[103] Chu PK, Li L. Characterization of amorphous and nanocrystalline carbon films. Materials Chemistry and Physics. 2006;**96**:253-277. DOI: 10.1016/j.matchemphys.2005.07.048

[104] Pradhan D, Lin IN. Grain-size-dependent diamond-nondiamond composite films: Characterization and field-emission properties. ACS Applied Materials & Interfaces. 2009;**1**:1444-1450. DOI: 10.1021/am9001327

[105] Yanchuk IB, Valakh MY, Vul AY, Golubev VG, Grudinkin SA, Feoktistov NA, et al. Raman scattering, AFM and nanoindentation characterisation of diamond films obtained by hot filament CVD. Diamond and Related Materials. 2004;**13**:266-269. DOI: 10.1016/j.diamond.2003.11.001

[106] Sharda T, Rahaman MM, Nukaya Y, Soga T, Jimbo T, Umeno M. Structural and optical properties of diamond and nano-diamond films grown by microwave plasma chemical vapor deposition. Diamond and Related Materials. 2001;**10**:561-567. DOI: 10.1016/S0925-9635(00)00390-3

[107] Yin Z, Akkerman Z, Yang BX, Smith FW. Optical properties and microstructure of CVD diamond films. Diamond and Related Materials. 1997;**6**:153-158. DOI: 10.1016/S0925-9635(96)00740-6

[108] Yang JX, Li CM, Lu FX, Chen GC, Tang WZ, Tong YM. Microstructure and fracture strength of different grades of freestanding diamond films deposited by a DC arc plasma jet process. Surface & Coatings Technology. 2005;**192**:171-176. DOI: 10.1016/j.surfcoat.2004.04.089

[109] Yang JX, Duan XF, Lu FX, Li CM, Zuo TC, Wang FL. The influence of dark feature on optical and thermal property of DC arc plasma jet CVD diamond films. Diamond & Related Materials. 2005;**14**:1583-1587. DOI: 10.1016/j.diamond.2005.03.010

[110] Calvani P, Bellucci A, Girolami M, Orlando S, Valentini V, Polini R, et al. Black diamond for solar energy

conversion. Carbon. 2016;**105**:401-407. DOI: 10.1016/j.carbon.2016.04.017

[111] Bangert U, Barnes R. Electron energy loss spectroscopy of defects in diamond. Physica Status Solidi (a). 2007;**204**:2201-2210. DOI: 10.1002/pssa.200675442

[112] Badzian A. The displacement disorder of atoms in diamond crystals revealed by X-ray imaging plate detector. Diamond & Related Materials. 2016;**69**:19-32. DOI: 10.1016/j.diamond.2016.07.004

[113] Zolotukhin AA, Ismagilov RR, Dolganov MA, Obraztsov AN. Morphology and Raman spectra peculiarities of chemical vapor deposition diamond films. Journal of Nanoelectronics and Optoelectronics. 2012;**7**:22-28. DOI: 10.1166/jno.2012.1210

[114] Miki H, Tsutsui A, Takeno T, Takagi T. Friction properties of partially polished CVD diamond films at different sliding speeds. Diamond & Related Materials. 2012;**24**:167-170. DOI: 10.1016/j.diamond.2012.01.004

[115] Mallik AK, Bysakh S, Pal KS, Dandapat N, Guha BK, Datta S, et al. Large area deposition of polycrystalline diamond coatings by microwave plasma CVD. Transactions of the Indian Ceramic Society. 2013;**72**:225-232. DOI: 10.1080/0371750X.2013.870768

[116] Mallik AK, Bysakh S, Pal KS, Dandapat N, Guha BK, Datta S, et al. Synthesis and characterisation of freestanding diamond coatings. Indian Journal of Engineering and Materials Science. 2013;**20**:522-532

[117] Mallik AK, Bhar R, Bysakh S. An effort in planarising microwave plasma CVD grown polycrystalline diamond (PCD) coated Si wafers of 4 inch diameter. Materials Science in Semiconductor Processing. 2016;**43**:1-7. DOI: 10.1016/j.mssp.2015.11.016

[118] Mallik AK, Mendes JC, Rotter SZ, Bysakh S. Detonation nanodiamond seeding technique for nucleation enhancement of CVD diamond—Some experimental insights. Advances in Ceramic Science and Engineering. 2014;**3**:36-45. DOI: 10.14355/acse.2014.03.005

[119] Mallik AK, Bysakh S, Bhar R, Rotter SZ, Mendes JC. Effect of seed size, suspension recycling and substrate pre-treatment on the CVD growth of diamond coatings. Open Journal of Applied Sciences. 2015;**5**:747-763. DOI: 10.4236/ojapps.2015.512071

[120] Determination of the Specific Surface Area of Solids by Gas Adsorption—BET Method. 2nd ed. BS ISO 9277:2010

[121] Pal KS, Mallik AK, Dandapat N, Ray NR, Datta S, Bysakh S, et al. Microscopic properties of MPCVD diamond coatings studied by micro-Raman and micro-photoluminescence spectroscopy. Bulletin of Materials Science. 2015;**38**:537-549. DOI: 10.1007/s12034-015-0860-9

[122] Tallaire A, Collins AT, Charles D, Achard J, Sussmann R, Gicquel A, et al. Characterisation of high-quality thick single-crystal diamond grown by CVD with a low nitrogen addition. Diamond & Related Materials. 2006;**15**:1700-1707. DOI: 10.1016/j.diamond.2006.02.005

[123] https://www.bruker.com/fileadmin/user_upload/8-PDF-Docs/OpticalSpectrospcopy/FT-IR/ALPHA/AN/AN81_Diamonds_EN.pdf [Accessed: 12th April, 2017]

[124] Tang CJ, Hou H, Fernandes AJS, Jiang XF, Pinto JL, Ye H. Investigation of bonded hydrogen defects in nanocrystalline diamond films grown with nitrogen/methane/hydrogen plasma at high power conditions. Journal of Crystal Growth. 2017;**460**:16-22. DOI: 10.1016/j.jcrysgro.2016.12.050

[125] Pezzagna S, Rogalla D, Wildanger D, Meijer J, Zaitsev A. Creation and nature of optical centres in diamond for single-photon emission—Overview and critical remarks. New Journal of Physics. 2011;**13**:035024. DOI: 10.1088/1367-2630/13/3/035024

[126] Schirhagl R, Chang K, Loretz M, Degen CL. Nitrogen-vacancy centers in diamond: Nanoscale sensors for physics and biology. Annual Review of Physical Chemistry. 2014;**65**:83-105. DOI: 10.1146/annurev-physchem-040513-103659

[127] Ulrika FS, D'Haenens-Johansson AK, Moe KS, Johnson P, Wang W. Large colorless HPHT-grown synthetic gem diamonds from new diamond technology. Russia, Gems & Gemology. 2015;**51**:3. Available from: https://www.gia.edu/gems-gemology/fall-2015-large-colorless-hpht-grown-synthetic-gem-diamond-technology-russiaFacebook48TwitterPrintEmailPinterestMore97

[128] Collins AT. Vacancy enhanced aggregation of nitrogen in diamond. Journal of Physics C: Solid State Physics. 1980;**13**:2641-2650. DOI: 10.1088/0022-3719/13/14/006

[129] Mallik AK, Bysakh S, Sreemany M, Roy S, Ghosh J, Roy S, et al. Property mapping of polycrystalline diamond coatings over large area. Journal of Advanced Ceramics. 2014;**3**:56-70. DOI: 10.1007/s40145-014-0093-1

[130] Oliver WC, Pharr GM. An improved technique for determining hardness and elastic modulus. Journal of Materials Research. 1992;**7**:1564-1583. DOI: 10.1557/JMR.1992.1564

[131] Jana A, Dandapat N, Das M, Balla VK, Chakraborty S, Saha R, et al. Severe wear behaviour of alumina balls sliding against diamond ceramic coatings. Bulletin of Materials Science. 2016;**39**:573-586. DOI: 10.1007/s12034-016-1166-2

[132] Almeida FA, Maru MM, Shabani M, Oliveira FJ, Silva RF, Achete CA. Enhancing the tribological performance under biodiesel lubrication using CVD diamond coated parts. Wear. 2013;**302**:1370-1377. DOI: 10.1016/j.wear.2013.01.090

[133] Shen B, Chen S, Chen Y, Sun F. Enhancement on the tribological performance of diamond films by utilizing graphene coating as a solid lubricant. Surface & Coatings Technology. 2017;**311**:35-45. DOI: 10.1016/j.surfcoat.2016.12.094

[134] Chen S, Shen B, Sun F. Tribo-map of CVD diamond film sliding against silicon nitride in air. Key Engineering Materials. 2014;**589-590**:405-410. DOI: 10.4028/www.scientific.net/KEM.589-590.405

[135] Bogatov A, Traksmaa R, Podgursky V. Changes in surface morphology, deflection and wear of microcrystalline diamond film observed during sliding tests against Si_3N_4 balls. Key Engineering Materials. 2016;**674**:145-115. DOI: 10.4028/www.scientific.net/KEM.674.145